Structure Transition and Tuning Pattern in the Double (Tetramethylammonium Hydroxide + Gaseous Guests) Clathrate Hydrates

Sukjeong Choi, Kyuchul Shin, and Huen Lee*

Department of Chemical and Biomolecular Engineering, Korea Advanced Institute of Science and Technology (KAIST), 373-1 Guseong-dong yuseong-gu, Daejeon 305-701, Republic of Korea

Received: May 21, 2007; In Final Form: July 2, 2007

In this study, we present an extraordinary structural transition accompanying the occurrence of more than two coexisting clathrate hydrate phases in the double (CH_4 + tetramethylammonium hydroxide (Me_4NOH)) and (H_2 + Me_4NOH) ionic clathrate hydrates using solid-state NMR spectroscopy (high-powered decoupling and CP/MAS) and powder X-ray diffraction. It was confirmed that structure-I (sI) and structure-II (sII) hydrates coexist as the water concentration increases. In the Me_4NOH-depleted region, the unique tuning phenomenon was first observed at a chemical shift of −8.4 ppm where relatively small gaseous CH_4 molecules partly occupy the sII large cages (sII-L), pulling out large cationic Me_4N^+ that is considered to be strongly bound with the surrounding host lattices. Moreover, we note that, while pure $Me_4NOH{\cdot}16H_2O$ clathrate hydrates melted at 249 K under atmospheric pressure conditions, the double (CH_4 + Me_4NOH) clathrate hydrate maintained a solid state up to approximately 283 K under 120 bar of CH_4 with a conductivity of 0.065 S cm^{-1}, suggesting its potential use as a solid electrolyte. The present results indicate that ionic contributions must be taken into account for ionic clathrate hydrate systems because of their distinctive guest dynamic behavior and structural patterns. In particular, microscopic analyses of ionic clathrate hydrates for identifying physicochemical characteristics are expected to provide new insights into inclusion chemistry.

Introduction

Unlike widely known non-ionic clathrate hydrates stabilized by van der Waals interactions between a host framework and a guest molecule,[1] ionic clathrate hydrates are a type of inclusion compound in which an ionic interaction exists between a cation or an anion guest and the surrounding host cage.[2] Various types of ionic molecules such as HPF_6, HBF_4, and alkyl ammonium salts are known to form their own structures of pure ionic clathrate hydrates without any cage occupancy by small gaseous guest molecules.[2−4] A number of notable studies on pure ionic clathrate hydrates has utilized their unique ionic characteristics for electric applications such as serving as the electrolyte for nickel−metal hydride batteries.[5,6] Pure or mixed non-ionic clathrate hydrates have also been examined mainly for versatile energy and environmental applications such as future energy resources, gas storage, and carbon dioxide sequestration.[7−10] Although quaternary ammonium salt hydrates have recently been applied to the area of gas separation and storage with the expectation of small co-guest occupancy in empty cages, most research has been oriented towards macroscopic approaches based on hydrate phase equilibria and process variables.[11,12] Ionic guests strongly interacting with the water cage framework make the resulting clathrate hydrate structure more complex than the hydrate structure of non-ionic guests. Moreover, several different crystalline phases of ionic clathrate hydrates are generally observed over the entire range of water concentrations.[4] Thus far, spectroscopic analyses for identifying the structure transition of ionic clathrate hydrates together with a comprehensive consideration of their complex phase patterns have not yet been reported in spite of the urgent need for them in inclusion chemistry.

In this study, an extraordinary structural transition and tuning mechanism occurring in cage-like as well as channel-like host frameworks of the double (CH_4 + tetramethylammonium hydroxide (Me_4NOH)) and (H_2 + Me_4NOH) ionic clathrate hydrates are first reported, and the channel-induced tuning phenomenon exchanging relatively large cations with small guest molecules is also examined. Me_4NOH hydrate has been the subject of some research, primarily owing to its peculiar structural characteristics, which are strongly influenced by the water concentration and temperature. $Me_4NOH{\cdot}nH_2O$ has been reported to have eight different crystalline hydrate phases according to its hydration number and temperature. Among these phases, β-forms of $Me_4NOH{\cdot}7.5H_2O$ (β-7.5 hydrate) and $Me_4NOH{\cdot}5H_2O$ (β-5 hydrate) are true ionic clathrate hydrates composed of an encaged Me_4N^+ cationic guest and a water host lattice in which the anions are incorporated by hydrogen bonding. The α-form hydrates also have a clathrate-related structure, but some of the oxygen atoms are not fully connected. Given that the β-form hydrates appear at a higher temperature as compared to the α-form hydrates, genuine clathrate hydrates do not exist at temperatures below 279 K.[2,4] The unusual structure patterns of ionic clathrate hydrates identified from solid-state NMR spectra were confirmed on the basis of powder X-ray diffraction (PXRD). In particular, the ionic conductivities of ionic clathrate hydrates were measured to examine their potential applications to energy devices.

Experimental Procedures

Reagents. The CH_4 and H_2 gases with a minimum purity of 99.95 mol % used in this study were supplied by Special Gas.

* Corresponding author. Fax: 82-42-869-3910; tel.: 82-42-869-3917; e-mail: h_lee@kaist.ac.kr.

10.1021/jp073910c CCC: $37.00
Published on Web 08/04/2007

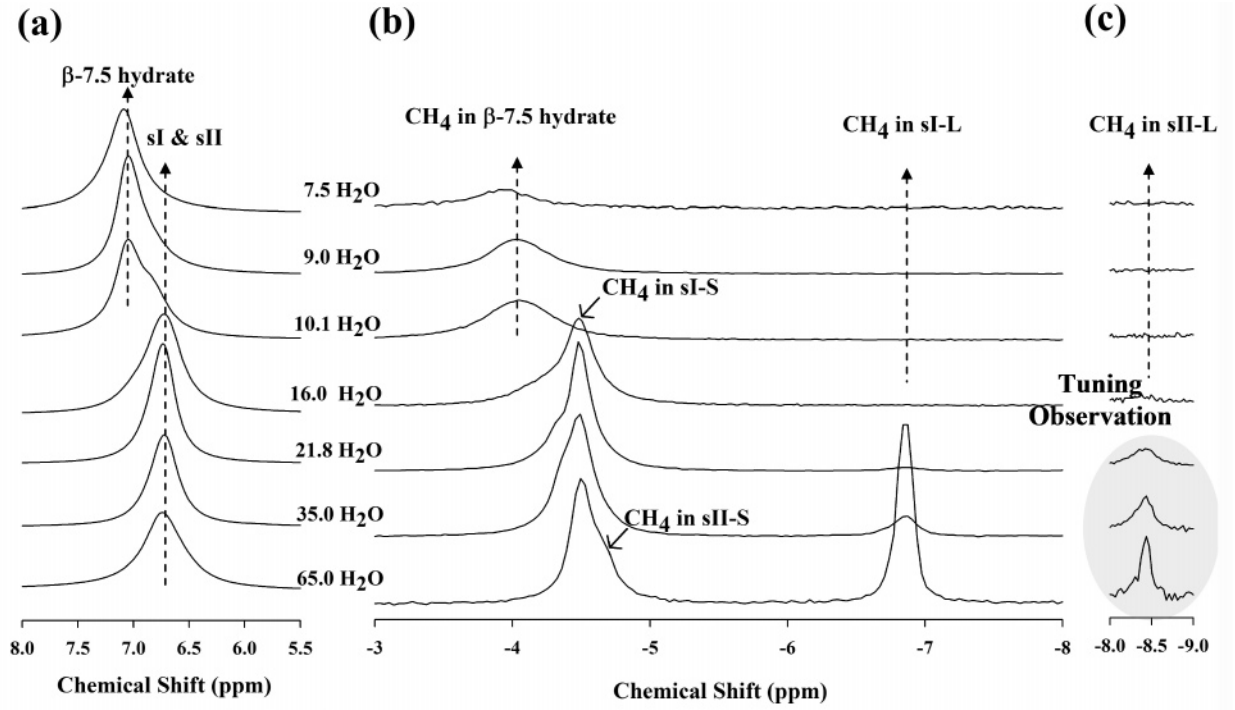

Figure 1. (a) ^{1}H MAS and (b) HPDEC ^{13}C NMR spectra of double (CH_4 + Me_4NOH) ionic hydrate system at 203 K and a 5 kHz spinning rate; $7.5H_2O$ means 7.5 mol of H_2O per 1.0 mol of Me_4NOH sample. (c) HPDEC ^{13}C NMR spectra between −8.0 and −9.0 ppm. Tuning pattern representing CH_4 occupancy in sII-L is clearly detected from a water concentration higher than $21.8H_2O$.

The $^{13}CH_4$ gas with a minimum purity of 99.0% was supplied by Cambridge Isotope Laboratories, Inc. Water of ultrahigh purity was supplied by Merck, and the tetramethylammonium hydroxide pentahydrate was supplied by Sigma-Aldrich, Inc. The tetramethylammonium hydroxide solutions were frozen at 203 K for at least 1 day and were then ground to a fine powder (∼200 μm). The powdered solid hydrate was placed in two pressurized cells each with a volume of 20 cm^3 and was then exposed to CH_4 or H_2 gas at a constant pressure of 120 bar and temperature of 203 K for 48 h. After the hydrate formation process was completed, the formed hydrate was finely powdered in the liquid nitrogen vessel.

Experimental Measurements. A Bruker Avance 400 MHz solid-state NMR spectrometer was used in this study. The powdered samples were placed in a 4 mm o.d. zirconia rotor loaded into a variable temperature probe. The ^{1}H NMR spectra of the (CH_4 + Me_4NOH) samples were recorded with magic angle spinning (MAS) at approximately 5 kHz, and the proton resonance peak of tetramethylsilane (TMS), assigned a chemical shift of 0 ppm at 298 K, was used as an external chemical shift reference. The ^{1}H NMR spectra of the (H_2 + Me_4NOH) samples were recorded with MAS at approximately 12 kHz to obtain sharper signals from the H_2 hydrates. All ^{13}C NMR spectra were recorded at a Larmor frequency of 100.6 MHz with MAS at approximately 5 kHz. A pulse length of 2 μs and a pulse repetition delay of 10 s under proton decoupling were employed with a radio frequency field strength of 50 kHz, corresponding to 5− μs 90° pulses. The downfield carbon resonance peak of adamantine was assigned a chemical shift of 38.3 ppm at 298 K and was used as an external chemical shift reference. The cross-polarization (CP) NMR spectra were also obtained to identify the gas and liquid phase signal from the high-power decoupling (HPDEC) NMR spectra. For the mixed hydrate samples, $^{13}CH_4$ was mixed to obtain higher intensity CH_4 signals.

The PXRD patterns were recorded at 203 K on a Rigaku D/MAX-2500 device using graphite-monochromatized Cu Kα1 radiation (λ = 1.5406 Å) in the $\theta/2\theta$ scan mode. The XRD experiments were carried out in step mode with a fixed time of 3 s and a step size of 0.03° for 2θ = 5 to 55 for each hydrate sample.

Ionic conductivities were analyzed via complex impedance analysis using a Solartron 1260A frequency response analyzer in a frequency range from 10 to 10^6 Hz. SUS electrodes with a surface area 0.625 cm^2 were separated by 0.2 cm using a Teflon plate.

Results and Discussion

Figure 1 represents the ^{1}H and HPDEC ^{13}C NMR spectra of double (CH_4 + Me_4NOH) ionic clathrate hydrates at several different water concentrations at a temperature of 203 K. The proton signals from the host lattice at all water concentrations are in Figure 1a. The entire spectra including Me_4N^+ and CH_4 signals are in Figure 2a. As shown in the ^{1}H NMR spectrum of the ice and water lattice framework of sI and sII (Figure 3), the resonance line width of the ice signal is very large due to strong dipolar coupling involving ^{1}H spins that are close together.[13] On the other hand, adding OH^- sharpens the resonance line width, and the peak is shifted downfield. This peak pattern implies that the anion (OH^-) strongly influences the sharpness of the H_2O signal. Therefore, signals ranging between δ = 6.7 and δ = 7.1 ppm (Figure 1a) are considered to be the host lattice signals of the ionic clathrate hydrates. The ^{13}C signal from CH_4 is presented in Figure 1b,c (the entire spectra including Me_4N^+ and gas phase signals are represented in Figure 2b; the CH_4 signals in the gas phase were identified by comparing with CP^{13}C NMR spectra (Figure 2c)).

A remarkable peak shifting appears in both ^{1}H and ^{13}C NMR spectra of the $16.0H_2O$ sample in Figure 1. In Figure 1a, the host lattice signal at δ = 7.1 ppm shifts to δ = 6.7 ppm around $16.0H_2O$ at which point the CH_4 signal shifts from δ = −4.0 ppm to δ = −4.5 ppm, leading to a structure transition of double (CH_4 + Me_4NOH) ionic hydrates. At water concentrations

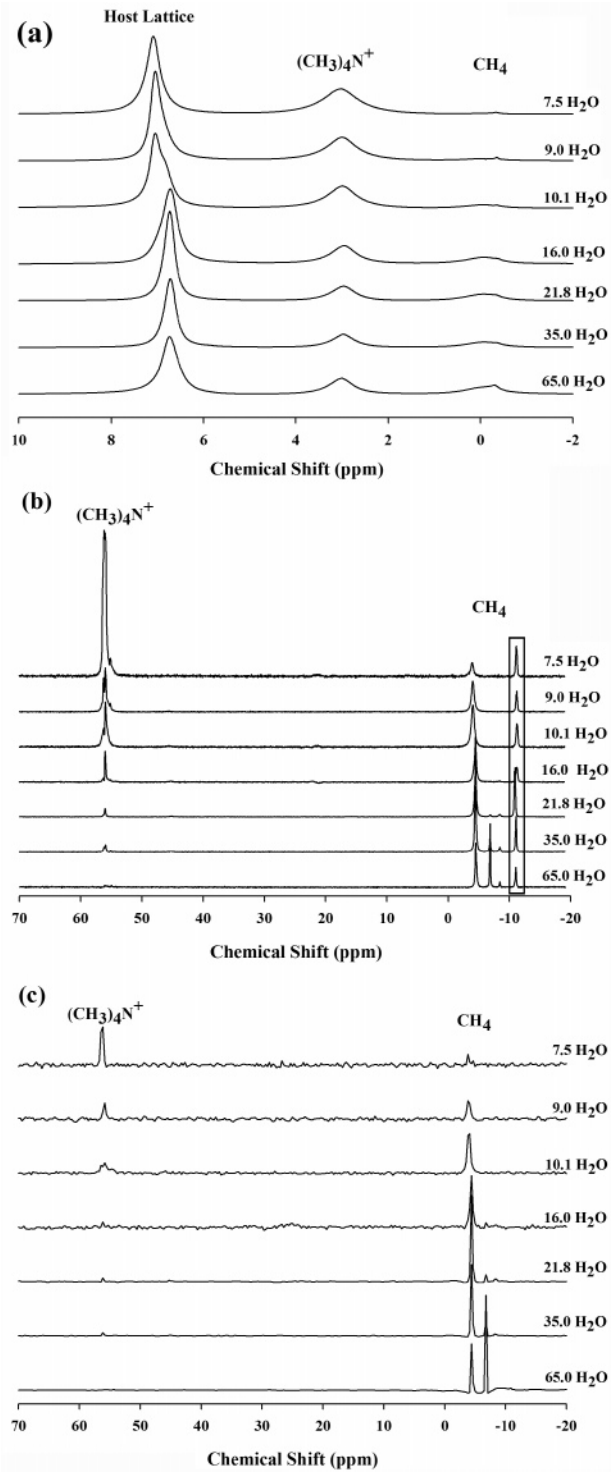

Figure 2. (a) Entire ^1H NMR spectra including Me_4N^+ and CH_4 signals. (b) Entire HPDEC ^{13}C NMR spectra including gas phase (black box) and Me_4N^+ signals. (c) CP/MAS ^{13}C NMR spectra. CH_4 signals in the gas phase (panel b: $\delta = -11.1$ ppm) were not observed.

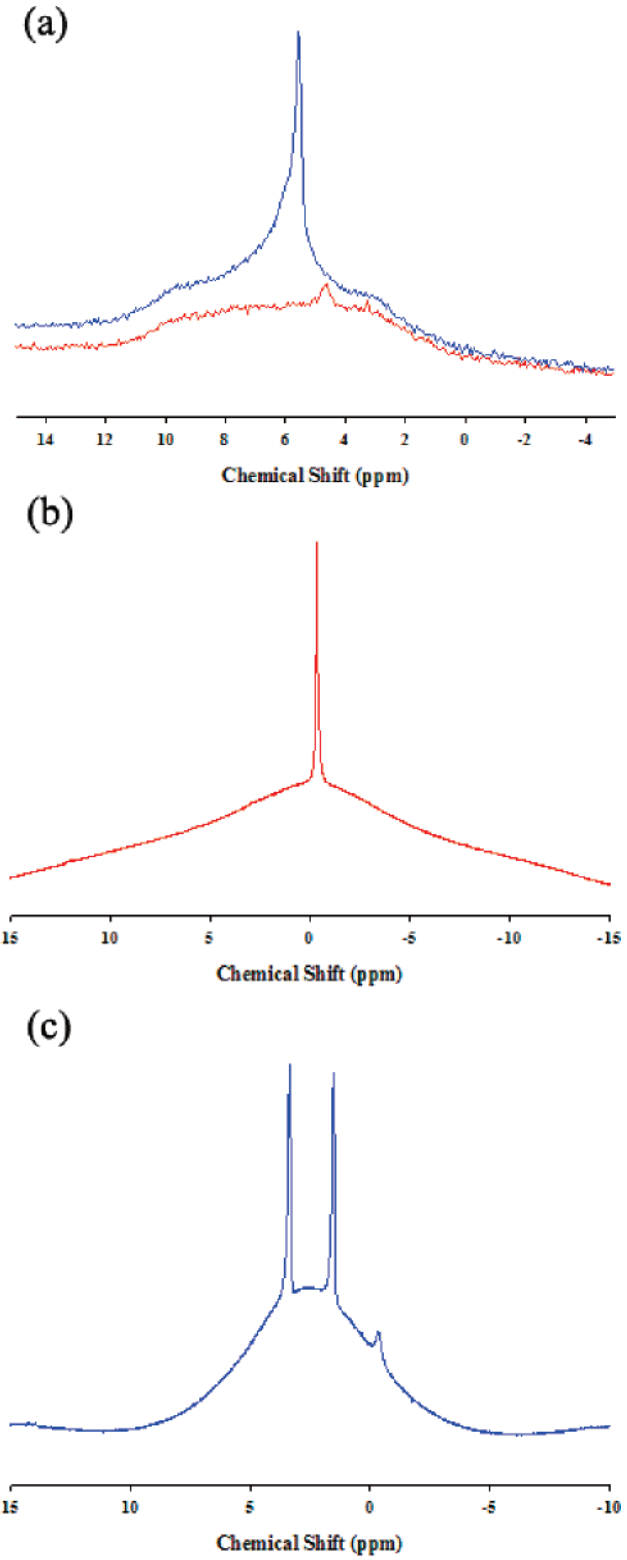

Figure 3. ^1H MAS NMR spectra of pure ice, ice + NaOH (16.5 mol %), sI, and sII hydrate. (a) Ice: red and (ice + NaOH) mixture: blue. (b) Pure CH_4 sI hydrate. (c) (Tetrahydrofuran + CH_4) sII hydrate.

higher than $16.0H_2O$, most of the β-7.5 ionic clathrate hydrate transforms to the sI. Here, it should be noted that this converted sI is the double ionic rather than the pure CH_4 clathrate hydrate simply formed by only water and methane. From the ^{13}C NMR spectra (Figure 1b), it is confirmed that nearly complete conversion to sI is achieved at water concentrations higher than 16.0 mol of H_2O per 1.0 mol of Me_4NOH ($16.0H_2O$). Significantly, small signals of CH_4 in large cages of sI (sI-L, $\delta = -6.9$ ppm) and sII hydrates (sII-L, $\delta = -8.4$ ppm),[14] as compared to ideal distributions of CH_4 in the sI and sII cages, imply that Me_4N^+ is enclosed in both sI-L and sII-L at a higher water concentration (Figure 1b; $16H_2O$, $21.8H_2O$, and $35H_2O$). However, the CH_4 signal at $\delta = -4.0$ ppm (Figure 1; $7.5H_2O$, $9.0H_2O$, and $10.1H_2O$) cannot be assigned solely by NMR spectra. This peak, which is located at a more deshielded region than CH_4 in small cages of sI (sI-S, $\delta = -4.5$ ppm) and sII (sII-S, $\delta = -4.7$ ppm),[14] indicates that CH_4 is enclosed in a smaller cage than sI-S and sII-S. Considering that only β-7.5

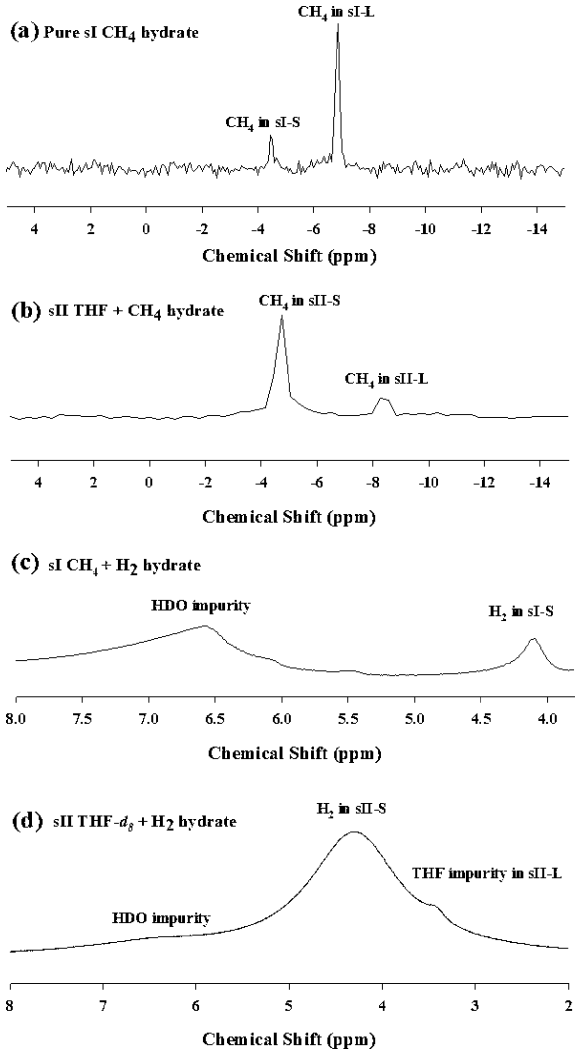

Figure 4. HPDEC ^{13}C NMR spectra of (a) pure sI CH_4 hydrate and (b) sII (THF + CH_4) hydrate. ^1H MAS NMR spectra of (c) sI (H_2 + CH_4) hydrate and (d) sII (THF-d_8 + H_2) hydrate. D_2O was used for ^1H NMR analysis.

TABLE 1: Average Radii of Clathrate Hydrate Cages (sI-S, sII-S, and β-7.5)

cage	av radius (Å)
β-7.5 hydrate ($4^2 5^8$)	3.46[4a]
sI-S (5^{12})	3.95[15]
sII-S (5^{12})	3.91[15]

[a] Value was calculated using atomic positions.

hydrate has an empty cage ($4^2 5^8$) that not only can be occupied by a CH_4 molecule but also is smaller than sI-S or sII-S among the eight crystalline phases of $Me_4NOH \cdot nH_2O$, β-7.5 hydrate is the most likely structure for low water concentration hydrates (Table 1).[4]

Another remarkable observation in the (CH_4 + Me_4NOH) clathrate hydrate system is the tuning phenomenon (Figure 1b, c). As seen in Figure 1b,c, a unique tuning phenomenon is clearly observed at a chemical shift of −8.4 ppm, where relatively small gaseous CH_4 molecules partly occupy the sII-L cages, pulling out large cationic Me_4N^+ that is considered to be strongly bound with the surrounding host lattices. Such a small and nonpolar guest inclusion into the sII-L cages of the ionic clathrate hydrate is a surprising feature from the viewpoint of inclusion chemistry.[10,16] First, it can be thought that the relatively small critical radii of the sII-S channels restrict the uptake of small guest

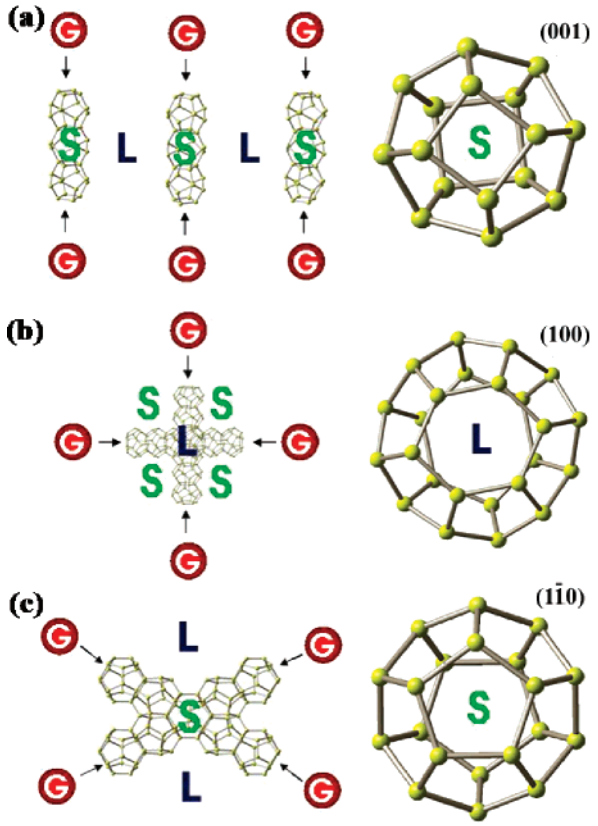

Figure 5. Channel patterns of guest diffusion pathways composed by like-cage stacking. Surrounding cages adjacent to the channels are irregularly arranged. (a) $4^2 5^8$ channel in the β-7.5 clathrate hydrate and $4^2 5^8$ channel entrance. (b) $5^{12}6^2$ channel in the sI clathrate hydrate and $5^{12}6^2$ channel entrance. (c) 5^{12} channel in the sII clathrate hydrate and 5^{12} channel entrance (G: guest; L: large cage; and S: small cage).

molecules. More significantly, the irregular and disordered sII-L polyhedral cages encompass the sII-S channels without any ice phase appearance when the mixed hydrate is formed at a stoichiometric proportion. However, even at the excess water concentration, only a small amount of the pure ice phase can coexist because most of the ice phase must be structurally transformed to pure methane clathrate hydrate. This sI structure naturally provides continuous small guest diffusion openings through intersecting sI-L channels, thus enabling small guest molecules to attack the cations encaged in sII-L through the windows of sI-L polygonal faces and eventually occupy the sII-L cages. Accordingly, such an unusual tuning mechanism is likely to be better understood through simultaneous consideration of channel-like as well as cage-like host framework characteristics. In a specific intra-crystalline clathrate hydrate structure, guest molecules of a suitable size and shape may be readily accessible to the resulting patterns of channels and cages, as observed in zeolite inclusion complexes. In Figure 5, three different channel patterns are shown for β-7.5, sI, and sII. The β-7.5 channels are all parallel, and thus, no cross-connecting openings for guest molecules to cross from one channel to adjacent channels exist, and only one-dimensional diffusion takes place. The polygonal faces provide windows essential for creating continuous diffusion paths for guest molecules or for exchangeable cations. Thus far, although the vacant channels formed by the linkage of specific cages have not received any attention in the inclusion phenomena of clathrate hydrates, it is essential to realize that these channels can play an important role in guest diffusion pathways and occupancy occurring in a complex clathrate hydrate matrix. Apparently, the presence of guest molecules in

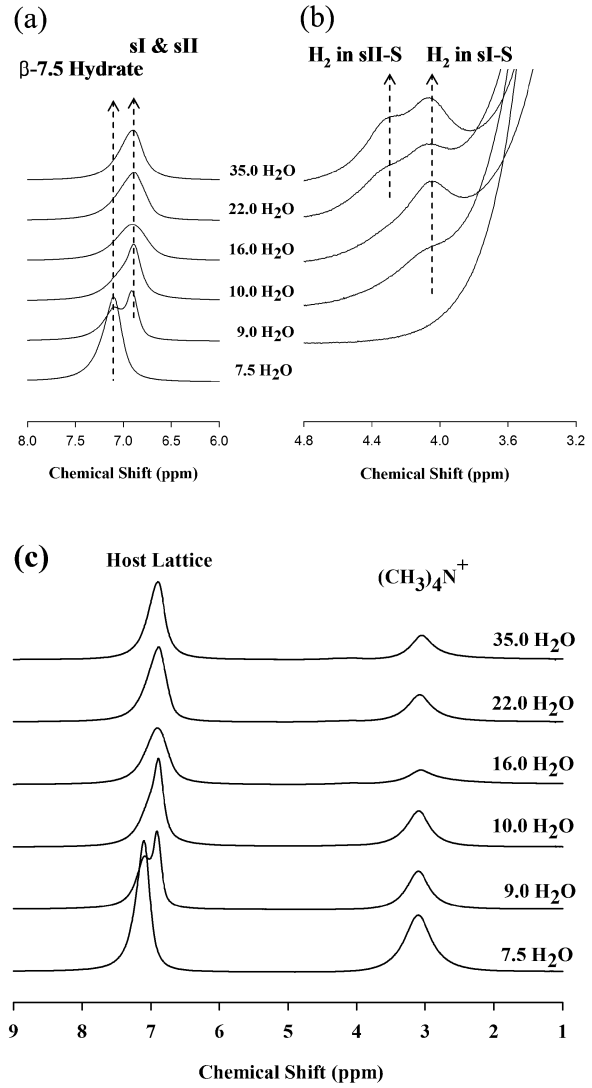

Figure 6. ^{1}H MAS NMR spectra of the double (H_2 + Me_4NOH) ionic clathrate hydrate measured at 203 K and a 5 kHz spinning rate. (a) Region of host lattice signal. (b) Region of H_2 signal. (c) Entire ^{1}H NMR spectra. Because H_2 peaks are too small as compared to Me_4N^+ signal, H_2 signals are not seen in these spectra.

the nearly immobile host frameworks is capable of inducing the crystalline structure to transform to a more stable structure by lowering the chemical potential of the fresh host lattice formation.

A similar structural pattern was observed in the double (H_2 + Me_4NOH) ionic clathrate hydrates as shown in Figure 6. The incipient signal shift of the host lattice is observed in the 9.0H_2O sample, which appears to be slightly lowered as compared to that of the (CH_4 + Me_4NOH) clathrate hydrate. The H_2 peaks representing sI-S (δ = 4.1 ppm) first appear, but under more hydrated surroundings, the H_2 peaks representing sII-S (δ = 4.3 ppm) are newly detected,[17] confirming the coexistence of two different sI and sII double (H_2 + Me_4NOH) ionic clathrate hydrates. Again, it is important that the sI phase only contains

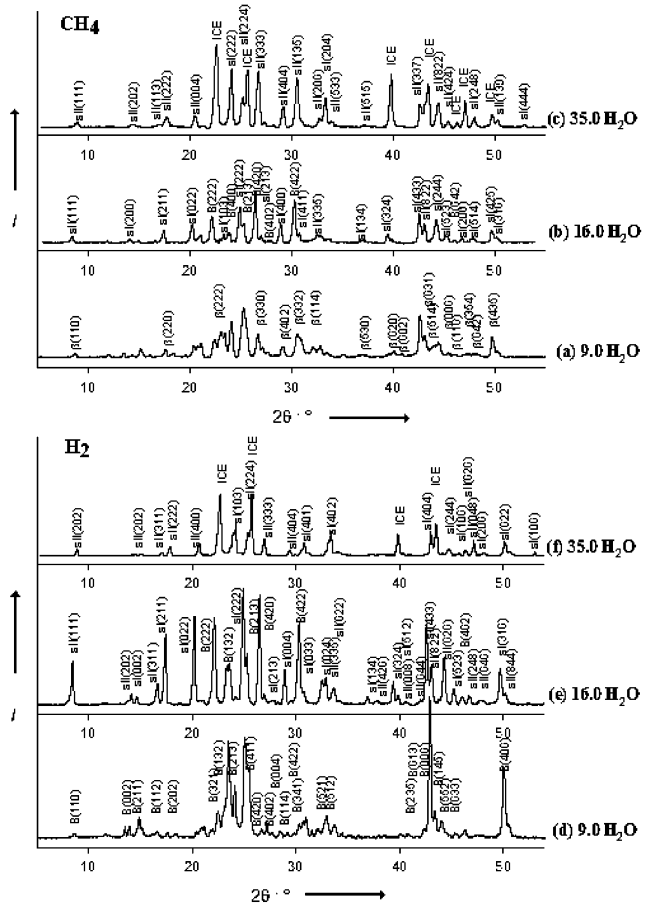

Figure 7. PXRD patterns of ionic hydrates enclosing gas guest. (Me_4-NOH + CH_4) clathrate hydrate samples: (a) 9.0H_2O sample, (b) 16.0H_2O sample, and (c) 35.0H_2O sample. (Me_4NOH + H_2) clathrate hydrate samples: (d) 9.0H_2O sample, (e) 16.0H_2O sample, and (f) 35.0H_2O sample. (B: β-7.5 hydrate; sI: structure-I hydrate; and sII: structure-II hydrate). Unlabeled peaks in spectra a and d indicate patterns of α-7.5 hydrate.

the double ionic clathrate hydrate, eliminating any possible formation of the pure hydrogen clathrate hydrate under the present experimental conditions. At excess water concentrations, most water molecules that do not participate in forming the ionic hydrate remain in the pure ice phase, hindering the creation of open windows through which hydrogen molecules must pass. As a result, one of the possible channels for approaching the sII-L cage does not exist in the (H_2 + Me_4NOH) hydrate system. The β-7.5 structure does not sufficiently provide potential cages or channels, which prevents H_2 molecules from migrating and becoming entrapped. This implies that the guest molecules with incongruent sizes and shapes become scarcely accessible and distributed to the empty confined space.

The ionic clathrate hydrate structures of the 9.0H_2O, 16.0H_2O, and 35.0H_2O samples were checked by PXRD and compared with the α-form of $Me_4NOH\cdot 7.5H_2O$ (α-7.5). The PXRD patterns were indexed by using the Checkcell program,[18] and determined unit cell parameters are described in Table 2. In

TABLE 2: Hydrate Crystal Cell Structures Determined by PXRD Patterns (Figure 7)

CH_4	type	crystal	space group	*a* (Å)	*c* (Å)	H_2	type	crystal	space group	*a* (Å)	*c* (Å)
a	β-7.5	tetragonal	*I*4/*mcm*	14.210	11.980	d	β-7.5	tetragonal	*I*4/*mcm*	14.210	11.980
b	β-7.5	tetragonal	*I*4/*mcm*	14.960	12.447	e	β-7.5	tetragonal	*I*4/*mcm*	14.960	12.447
	sI	cubic	*Pm*3*n*	12.412			sI	cubic	*Pm*3*n*	12.384	
	sII	cubic	*Fd*3*m*	17.832			sII	cubic	*Fd*3*m*	17.800	
c	sI	cubic	*Pm*3*n*	12.001		f	sI	cubic	*Pm*3*n*	11.942	
	sII	cubic	*Fd*3*m*	17.300			sII	cubic	*Fd*3*m*	17.271	

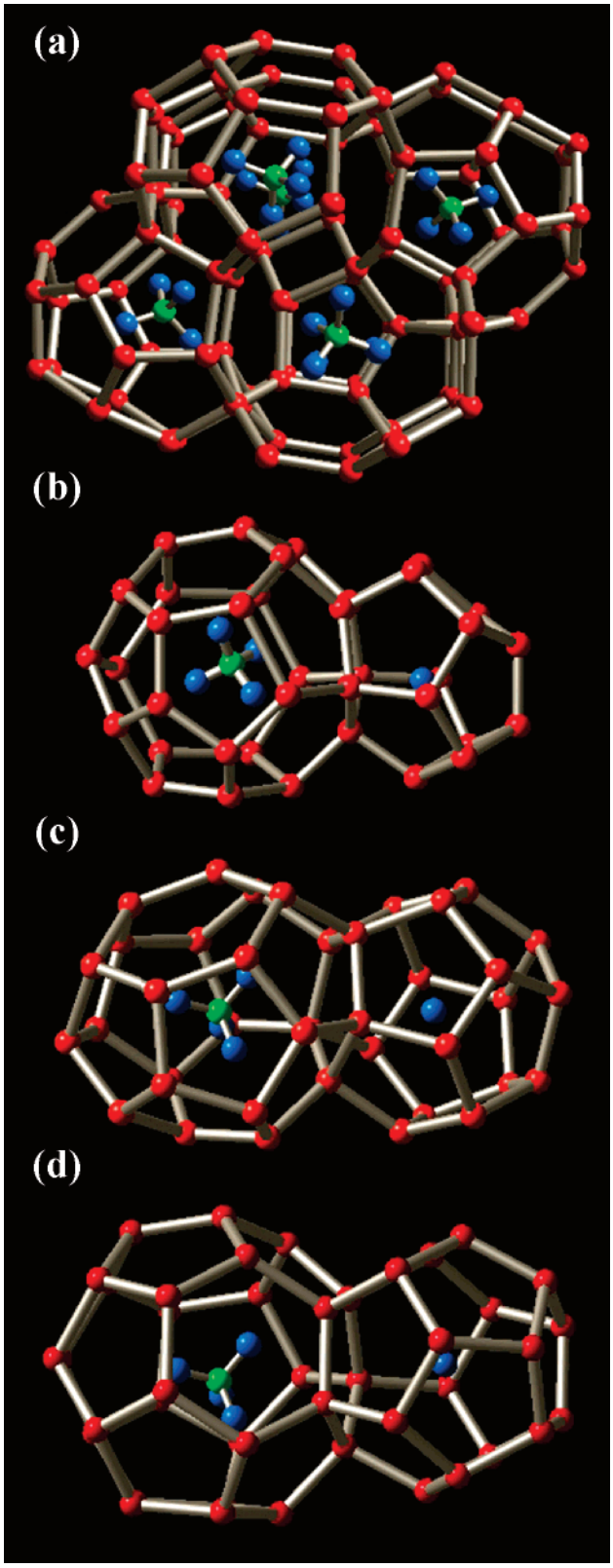

Figure 8. Structure of clathrate hydrate phases (a) α-7.5 hydrate[4], (b) *β*-7.5 hydrate, (c) double ($Me_4NOH + CH_4$) sI hydrate, and (d) double ($Me_4NOH + CH_4$) sII hydrate. Methane guest is represented by a single blue ball and Me_4N^+ guest by the blue and green balls. Structure is suggested from results of PXRD pattern indexing and from the analysis of ^1H and ^{13}C NMR results.

Figure 7a, the PXRD patterns of the ($CH_4 + Me_4NOH$) *β*-7.5 hydrate are detected, and thus, the *β*-7.5 hydrate, including the CH_4 in the (4^25^8) cage, is considered to coexist with the α-7.5 hydrate in the $9.0H_2O$ sample. In contrast, the PXRD patterns

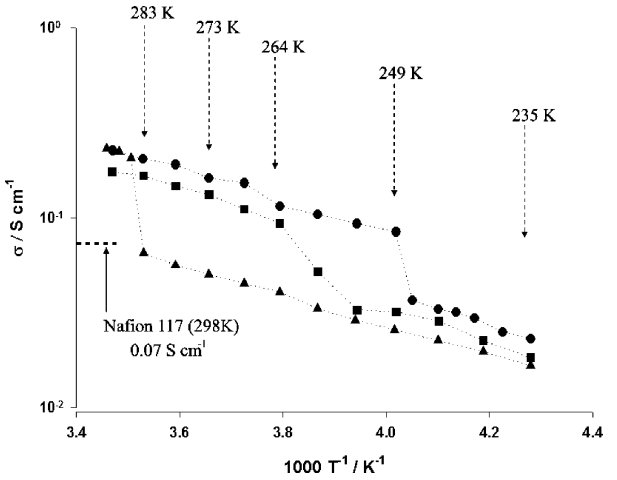

Figure 9. Ionic conductivities of pure Me_4NOH and double ($CH_4 + Me_4NOH$) ionic clathrate hydrates at various temperatures: (triangles) double ($CH_4 + Me_4NOH$)·$16.0H_2O$; (circles) pure Me4NOH·$16.0H_2O$; and (squares) pure Me_4NOH·$10H_2O$ clathrate hydrates.

of the $16.0H_2O$ and $35.0H_2O$ samples (Figure 7b, c) indicate that sI and sII become dominant as the water concentration increases, which is also clearly shown in Figure 1b. The double ($H_2 + Me_4NOH$) ionic clathrate hydrate system has similar PXRD patterns (Figure 7d−f). The PXRD patterns and NMR spectra reveal the complex structure transition of the double ($CH_4 + Me_4NOH$) and ($H_2 + Me_4NOH$) ionic clathrate hydrate according to the water concentration. Through the complex nature of this structure transition, it can be observed that the four solid hydrate phases of α-7.5, *β*-7.5, sI, and sII coexist (each structure is represented in Figure 8). It is noted from the ^{13}C NMR spectrum of the $65.0H_2O$ sample in Figure 1b and from the ^1H NMR spectrum of the $35.0H_2O$ sample in Figure 6b that the CH_4 and H_2 peak intensities representing sII-S increase. Close examination of the HPDEC ^{13}C and ^1H NMR spectra reveals that the type-II structure of the double ($CH_4 + Me_4NOH$) and ($H_2 + Me_4NOH$) ionic clathrate hydrates increases as the water concentration becomes higher. However, at water concentrations slightly higher than 10.0 mol of H_2O per 1.0 mol of Me_4NOH ($10H_2O$), sI appears to be dominant and gradually transforms to sII in proportion to the water concentration. This unusual structure transformation implies that the cationic and spherical-like Me_4N^+ guest is best incorporated in sII-L.

Another notable feature concerning the ionic clathrate hydrates is their potential application to solid electrolytes. Accordingly, the ionic conductivities of pure Me_4NOH and double ($CH_4 + Me_4NOH$) clathrate hydrates were measured. The results are represented in Figure 9. A specific water concentration of $16.0H_2O$ was especially chosen because the sI mixed ionic clathrate hydrate exists in excess at this concentration, while only very small amounts of other sII, 7.5-*β*, and 7.5-α phases can be detected in the solid solution. Thus, it becomes evident that the double ionic sI controls the overall ionic conductivity. For comparison, the conductivities of pure $10.0H_2O-Me_4NOH$ and $16.0H_2O-Me_4NOH$ hydrates were also measured, in which the $10H_2O$ is known to have the highest ionic conductivity among pure Me_4NOH hydrates.[19,20] The ionic conductivity of the $10H_2O$ at a solid-state ranged between 0.018 and 0.029 S cm^{-1} with an activation energy of 0.15 eV. Considering that the conductivity of Nafion 117, a commercial electrolyte, is 0.070 S cm^{-1} at 298 K,[21] $10H_2O$ exhibits an excellent conductivity as a proton or ionic conductor but simultaneously demonstrates an undesirable feature as an electrolyte due to its

low melting point (253 K). It is recalled that the liquid electrolytes are more difficult to handle than the solid electrolytes in terms of their application areas. However, for the double (CH_4 + Me_4NOH) clathrate hydrate with $16.0H_2O$, it maintains a solid state up to approximately 283 K with a conductivity of 0.065 S cm^{-1}, while the pure Me_4NOH hydrate melts at a lower temperature than the $10H_2O$. This considerable melting temperature increase to a point near ambient temperatures implies that ionic Me_4NOH clathrate hydrates incorporated with energy sources such as CH_4 might provide positive merits for the application to ionic conducting solid materials.

Conclusion

In this study, the effects of cations, anions, and water host molecules on the structural transition, tuning pattern, and ionic conductivity of double ionic clathrate hydrates occurring in confined cages as well as open channels were examined. However, macroscopic and microscopic approaches must be linked together to obtain a complete understanding of the guest dynamic behavior and host−guest interactions in the solid ionic state. It must be clearly understood that the inclusion phenomena and structural patterns of ionic clathrate hydrates are to a certain extent different from conventional non-ionic patterns, and thus, distinctive features due to ionic contributions must be taken into account. In particular, intra-crystalline channel patterns created in complex ionic host−guest networks are considered to play an important role in providing pathways and windows for small guest diffusion and sorption. Although several key structural and dynamic characteristics occurring in a crystalline clathrate hydrate matrix were addressed, further extensive works should be performed for versatile ionic clathrate hydrates with specific functions including ionic liquids and ionic surfactants[22] to promote a wider range of practical applicability. Furthermore, microscopic analyses of ionic clathrate hydrates that seek to identify physicochemical characteristics are expected to provide new insights into inclusion chemistry fields.

Acknowledgment. This research was supported by the Korea Science and Engineering Foundation (KOSEF) through the National Research Lab. Program funded by the Ministry of Science and Technology (R0A-2005-000-10074-0(2007)) and also was partially supported by the Brain Korea 21 Project.

References and Notes

(1) Platteeuw, J. C.; van der Waals, J. H. *Mol. Phys.* **1958**, *1*, 91−96.
(2) Jeffrey, G. A. *Inclusion Compounds*; Academic Press: London, 1984; Vol. 1.
(3) Mootz, D.; Oellers, E.-J.; Wiebcke, M. *J. Am. Chem. Soc.* **1987**, *109*, 1200−1202.
(4) Mootz, D.; Seidel, R. *J. Incl. Phenom.* **1990**, *8*, 139−157.
(5) Kuriyama, N.; Sakai, T.; Miyamura, H.; Kato, A.; Ishikawa, H. J. *Electrochem. Soc.* **1990**, *137*, 355−356.
(6) Kuriyama, N.; Sakai, T.; Miyamura, H.; Kato, A.; Ishikawa, H. *Solid State Ionics* **1990**, *40*−*41*, 906−909.
(7) Park, Y.; Kim, D.-Y.; Lee, J.-w.; Huh, D.-G.; Park, K.-P.; Lee, J.; Lee, H. *Proc. Natl. Acad. Sci. U.S.A.* **2006**, *103*, 12690−12694.
(8) Hailong, L.; Seo, Y.-t.; Lee, J.-w.; Moudrakovski, I.; Ripmeester, J. A.; Chapman, N. R.; Coffin, R. B.; Gardner, G.; Pohlman, J. *Nature* **2007**, *445*, 303−306.
(9) Yeon, S.-H.; Seol, J.; Lee, H. *J. Am. Chem. Soc.* **2006**, *128*, 12388.
(10) Kim, D.-Y.; Lee, J.-w.; Seo, Y.-t.; Ripmeester, J. A.; Lee, H. *Angew. Chem., Int. Ed.* **2005**, *44*, 7749−7752.
(11) Kamata, Y.; Oyama, H.; Shimada, W.; Ebinuma, T.; Takeya, S.; Uchida, T.; Nagao, J.; Narita, H. *Jpn. J. Appl. Phys.* **2004**, *43*, 362−365.
(12) Chapoy, A.; Anderson, R.; Tohidi, B. *J. Am. Chem. Soc.* **2007**, *129*, 746−747.
(13) Clayden, N. J.; Esposito, S.; Pernice, P.; Aronne, A. *J. Mater. Chem.* **2002**, *12*, 3746−3753.
(14) Peak positions of CH_4 in sI and sII hydrates were obtained from the pure CH_4 and mixed (tetrahydrofuran + CH_4) clathrate hydrates. These spectra are shown in Figure 4a,b.
(15) Sloan, E. D. *Clathrate Hydrates of Natural Gases*, 2nd ed.; Marcel Dekker, Inc.: New York, 1998.
(16) Kim, D.-Y.; Park, J.; Lee, J.-w.; Ripmeester, J. A.; Lee, H. *J. Am. Chem. Soc.* **2006**, *128*, 15360−15361.
(17) Peak positions of H_2 in sI-S and sII-S were obtained from the mixed (H_2 + CH_4) and (H_2 + tetrahydrofuran) clathrate hydrates. These spectra are shown in Figure 4c,d.
(18) Laugier, J.; Bochu, B. Laboratorire des Materiaus et du Genie Physique, Ecole Superieure de Physique de Grenoble; http://www.ccp14.ac.uk.
(19) Borkowska, Z.; Tymosiak, A.; Opallo, M. *J. Electroanal. Chem.* **1996**, *406*, 109−117.
(20) Borkowska, Z.; Opallo, M.; Tymosiak, A.; Zoltowski, P. *Colloids Surf., A* **1998**, *134*, 67−73.
(21) Reike, P. C.; Vanderborgh, N. E. *J. Membr. Sci.* **1987**, *32*, 313−328.
(22) Lee, S.; Zhang, J.; Mehta, R.; Woo, T.-K.; Lee, J. W. *J. Phys. Chem. C* **2007**, *111*, 4734−4739.